Review of Palaeobotany and Palynology 293 (2021) 104485

Contents lists available at ScienceDirect

Review of Palaeobotany and Palynology

journal homepage: www.elsevier.com/locate/revpalbo

Late Miocene *Cymodocea* seagrass in the Guadalquivir Basin (southern Spain)

Juan C. Braga [a,*], Ildefonso Bajo-Campos [b], Joaquín Cárdenas-Carretero [b]

[a] Departamento de Estratigrafía y Paleontología, Universidad de Granada, Campus Fuentenueva, 18002 Granada, Spain
[b] Museo de Alcalá de Guadaíra (Sección de Paleontología), C/ Juez Pérez Díaz, s/n, 41500 Alcalá de Guadaíra, Sevilla, Spain

ARTICLE INFO

Article history:
Received 14 March 2021
Received in revised form 1 July 2021
Accepted 2 July 2021
Available online 7 July 2021

Keywords:
Alismatales
Seagrass macrofossils
Paleoenvironment
Messinian
Alcalá de Guadaíra

ABSTRACT

Despite the abundance of seagrass-related deposits in the geological record, seagrass macrofossils are scattered in time and space, due to the low preservation potential of marine angiosperms. Fossil seagrass impressions, mainly rhizomes occur in Messinian (late Miocene) marl beds intercalated in cross-bedded bioclastic limestones in the Guadalquivir Basin near Alcalá de Guadaíra in southern Spain. Vegetative characters indicate that most remains can be attributed to *Cymodocea* cf. *nodosa*, to which also probably belong a few molds of fruits. Two other fossil fragments can only be assigned to Alismatales indet. The plants lived in sheltered ephemeral areas among shallow-water submarine dunes, in which deposition of fine-grained sediment favored their fossilization. During the late Miocene the Guadalquivir Basin was open to the Atlantic Ocean and, therefore, these fossil occurrences lie within the modern biogeographic distribution of *C. nodosa*, the only species of the genus out of the Indo-West Pacific region. At the moment, it is the only record of seagrass fossils in the Miocene of Europe.

1. Introduction

Seagrass fossils are rare and dispersed in time and space. The oldest records are from the Upper Cretaceous (early Campanian, ca. 82.5 Ma) of the southeast Netherlands, *Thalassocharis muelleri*. Relatively common silicified stems with roots and rarer leaf remains of seagrasses occur in Upper Cretaceous formations from Belgium and the Netherlands (Van der Ham et al., 2007, 2017; Jagt et al., 2019), and Germany (Van der Ham et al., 2007) in western Europe. Seagrass leaves and rhizomes have also been described in the Maastrichtian of Tennessee, USA (Dilcher, 2016). Eocene seagrass macrofossils are known from several localities in England, Belgium, France, Germany and Italy (Reich et al., 2015; Larkum et al., 2018 and references therein) as well as from the Avon Park Formation in Florida, USA (Benzecry and Brack-Hanes, 2008 and references therein). No seagrass macrofossils have been reported from Oligocene deposits and the only Miocene records so far described are from Sulawesi, Indonesia (Laurent and Laurent, 1926; Reich et al., 2015) and from the late Miocene in South Island, New Zealand (Larkum et al., 2018). External molds of seagrass leaves in basal surfaces of encrusting bryozoans (bioimmuration) are known from the Burdigalian in India (Reuter et al., 2010) and from the Mio-Pliocene of the Dominican Republic (Cheetham and Jackson, 1996). Pliocene macrofossils are also scarce and found in very distant localities. Fossil fruits were recorded in northern Italy (Ruggieri, 1951), a rich concentration of *Posidonia* leaves and rhizomes was found in the late Pliocene of Rhodes Island in Greece (Moissette et al., 2007), Larkum et al. (2018) illustrate Pliocene leaves from North Island, New Zealand, and Tuya et al. (2017) report *Halodule* rhizomes from the Canary Islands.

The oldest seagrass macrofossils were allied to the Cymodoceaceae–Zosteraceae–Posidoniaceae clade (Van der Ham et al., 2007). Some of the Eocene seagrasses both from western Europe and Florida were attributed to *Cymodocea* (Lumbert et al., 1984; Benzecry and Brack-Hanes, 2008 and references therein), the Miocene plants from Sulawesi and the Pliocene fruits from Italy (Ruggieri, 1951) were also attributed to this genus. *Cymodocea*, therefore, seems to have a long evolutionary history, although there is some uncertainty of the fossil affinities (Iles et al., 2015).

As can be seen in the above listed records no seagrass macrofossils have been found in European Oligocene to Miocene rocks despite the many references to seagrass-related deposits based on indirect indicators (Reich et al., 2015; Brandano et al., 2019, and references therein). These references include a number of late Miocene localities in the Betic Neogene basins in southern Spain, in which the occurrence of seagrass was interpreted from the benthic foraminifer assemblages (Brachert et al., 1998; Betzler et al., 2000; Puga-Bernabéu et al., 2007), coralline algal morphology and assemblages (Sola et al., 2013), and sediment features of (Betzler et al., 2000) of carbonate units.

In this paper, a concentration of seagrass macrofossils and its paleoenvironment of formation in Messinian (late Miocene) deposits in the Guadalquivir Basin in southern Spain are described. The fossil plant assemblage is nearly monospecific and, although no flowers or

* Corresponding author.
E-mail address: jbraga@ugr.es (J.C. Braga).

https://doi.org/10.1016/j.revpalbo.2021.104485

complete fruits are preserved vegetative characteristics indicate they belong to *Cymodocea*. This is the first record of Miocene seagrass macrofossils in Europe and adds a new site to the scarce number of known marine angiosperm vegetative fossils.

2. Location and geological setting

The site is located north of Alcala de Guadaíra, in the Sevilla province in southern Spain (Fig. 1). The fossiliferous beds occur in two of four pinnacles of poorly cemented limestone preserved from the extensive extraction of limestone gravel in an abandoned quarry (Latitude 37° 21′ 29″ N to 37° 21′ 34″ N, Longitude 5° 50′ 21″ W to 5° 50′ 26″ W, Figs. 1, 2). From a geological point of view, the locality is at the southern margin of the Guadalquivir Basin, the foreland basin of the Betic Cordillera, the westernmost peri-Mediterranean Alpine orogen (Fig. 1A). The Guadalquivir Basin originated during the Miocene by the tectonic flexure of the Iberian margin, due to nappe stacking in the frontal wedge of the Betic Cordillera at the southern active margin (Fernàndez et al., 1998; García-Castellanos et al., 2002). In the middle Miocene, olistostrome deposits from the Betic front mixed with autochthonous sedimentation, reaching the basin axis (Sanz de Galdeano and Vera, 1992). Along the southern margin, marine sedimentation took place on top of the accretionary wedge of the Betic Cordillera during the late Miocene. In the Alcalá de Guadaíra area, the upper Miocene marine deposits include blue marls at the base (Ecija Formation, Verdenius, 1970), followed by sandy silts with abundant glauconite (Transition Unit, Galán Huertos and Pérez Rodríguez, 1989), and bioclastic limestones with interspersed thin marl beds (Guadaíra Formation, Verdenius, 1970; Alcor Formation, Viguier, 1974). The fossil beds that are the subject of this study belong to the latter unit (Fig. 1B). The presence of *Globorotalia miotumida* and *Globorotalia margaritae* in the planktonic foraminifer assemblages indicates a late Messinian age for the Guadaíra Formation (Aguirre et al., 2015; González-Delgado et al., 2004; Perconig, 1968; Sierro et al., 1996). The succession from the Ecija to the Guadaíra formations constitutes the Andalusia Depositional Sequence, one of the stratigraphic sequences into which the sedimentary fill of the Guadalquivir Basin was divided (Martínez del Olmo and Martín, 2016, 2019).

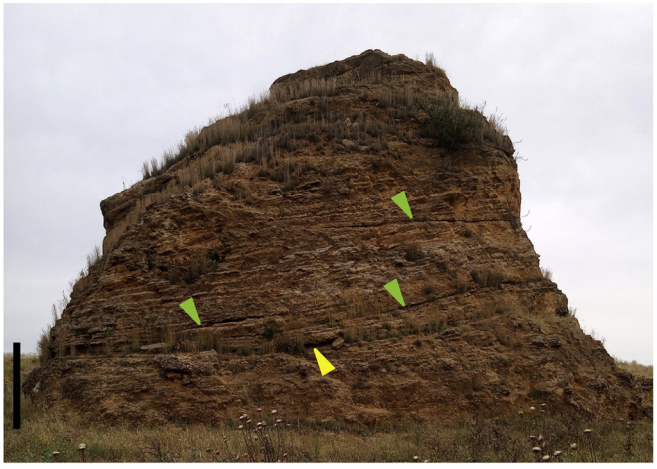

Fig. 2. View from south of the pinnacle preserved from limestone extraction in the Pie Solo quarry, in which the fossiliferous marl bed (yellow arrowhead) is exposed. Marl beds (green arrowheads) intercalate and pinch out among cross-bedded bioclastic grainstones to rudstones. Scale bar = 5 m.

3. Materials and methods

Ninety-eight samples of marl each containing one to many fossil fragments of seagrass were collected from the study site. The majority of samples were consolidated with a solution of 3% REGALREZ 1126 resin in ligroin. Voucher specimens are stored in the herbarium of the University of Granada (GDA). The rest of samples are stored in the Museo de Alcalá de Guadaíra (Sección Paleontología).

A sample of marl was washed for examination of its foraminifer content, using meshes of 0.5 and 0.125 mm, and then dried up in an oven at 40 °C. Only the residue in the 0.125 mm fraction was studied. The mineralogical composition of two samples of marl with fossil fragments was identified using X-ray diffraction. The elemental analyses were obtained with a Dual EDS (energy dispersive X-ray spectroscopy) system coupled

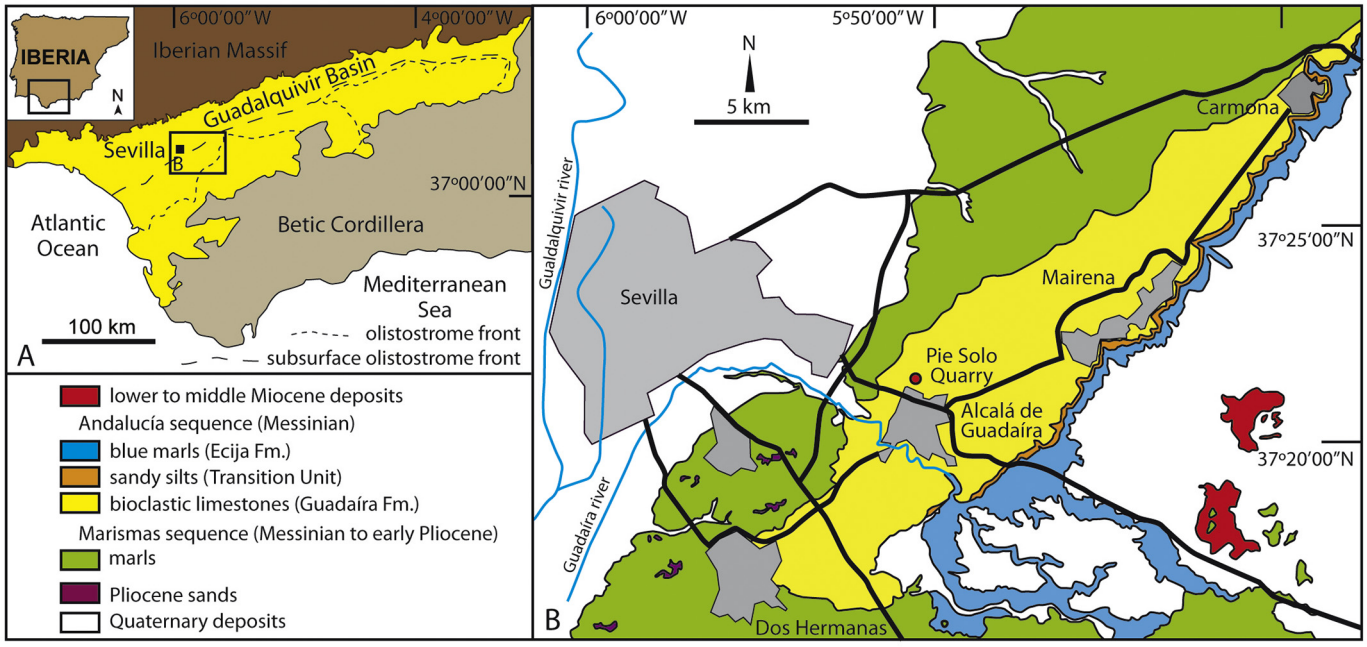

Fig. 1. A, Location of the study site in the Guadalquivir Basin in southern Spain. Inset shows area in B. B, Geological setting of the Pie Solo quarry, north of Alcalá de Guadaíra with main road access (black lines) and densely populated areas (gray polygons).

to an environmental scanning electron microscope (ESEM), Qemscan 650FEG (Thermofisher-FEI). The EDS detectors are Bruker XFlash 6/30 SDD (Silicon drift detector). The analyses were processed by the ESPRIT software at the "Centro de Instrumentación Científica" (CIC, Universidad de Granada). Four thin sections were cut from limestones above and below the fossiliferous marl beds to perform petrographic analysis of carbonates.

4. Results

4.1. Pie Solo section

Sample collection focused on one of the pinnacles in the quarry in which two marl beds with fossil plants are exposed (Figs. 2, 3). The pinnacle section begins with poorly exposed, trough cross-bedded grainstones to rudstones, up to 4 m thick. These beds are overlain by an interval, 1 m thick, of amalgamated rudstone lenses with erosive base and rough normal gradation. Individual lenses are some meters wide (up to 15 m, the lateral extent of the outcrop) and centimeters to decimeters in thickness. The rudstone consists of centimeter-sized, randomly oriented bioclasts with sharp edges in a packstone matrix with quartz grains. The bioclasts are mainly disarticulated bivalves and echinoids (Table 1), and minor gastropods, scaphopods, serpulids, barnacles, and fish teeth. The rudstone lenses laterally interfinger with trough cross-bedded laminated grainstone to rudstone.

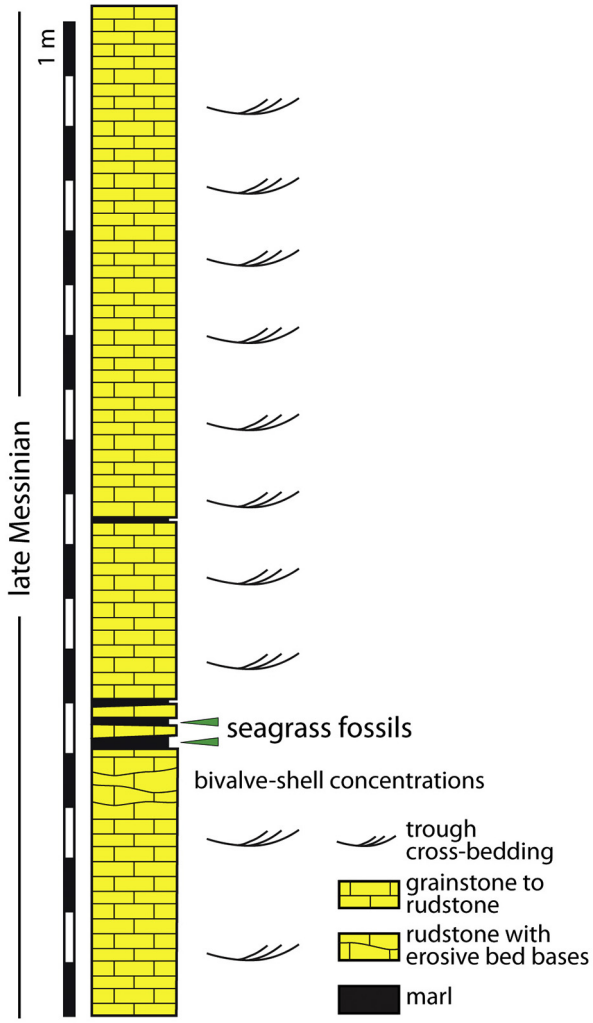

Fig. 3. Stratigraphic column of the Pie Solo section.

Table 1
Macroinvertebrates and trace fossils in the bioclastic limestones from the Pie Solo section, and foraminifers in the marl bed with seagrass macrofossils.

Bivalves	
Gigantopecten latissimus (Brocchi, 1814)	
Aequipecten scabrellus (Lamarck, 1819)	
Flabellipecten expansus (Sowerby, 1847)	
Oppenheimopecten praebenedictus Tournouër, 1920	
Pecten benedictus Lamarck,1819	
Ostrea edulis lamellosa (Brocchi,1814)	
Anomia ephippium Linnaeus,1758	
Glycymeris insubrica (Brocchi,1814)	
Modiolus adriaticus Lamarck,1819	
Limaria tuberculata (Olivi,1815)	
Gastropods	
Epitonium turtonis (W. Turton,1819)	
Echinoids	
Schizechinus duciei (Wright, 1855)	
Psammechinus dubius (Agassiz, 1840)	
Arbacina catenata (Desor, in Agassiz & Desor, 1846)	
Rhabdobrissus costae (Gasco, 1876)	
Echinocyamus sp.	
Annelids	
Serpula sp.	
Trace fossils	
Entobia	
Sinusischnus sinuosus	
Bichordites	
Foraminifera	%
Elphidium sp.	35.8
Biastigerinata sp.	20
Lobatula sp.	16.5
Cibicidoides sp.	10
Ammonia sp.	7
Florilus sp.	5.3
Planorbulina sp.	1
Uvigerina sp.	<1
Pullenia sp.	<1
Other benthic	<1
Planktonic	3.5

The interval is followed by a 10-cm-thick rippled rudstone with packstone matrix with up to 15% of quartz grains. Bivalve fragments are the main components, with secondary small benthic foraminifers, hooked and tubular coralline red algae, and bryozoans. Valve fragments show a preferred concordant convex-up orientation. This thin bed gives way to a marl bed, 10–16 cm in thickness, rich in the fossil marine angiosperms that are the subject of this report (see below). The marl bed is overlain by trough cross-bedded rudstones to coarse grainstones, with bed sets decimeters to a few meters thick and a total thickness of 12 m. The majority of beds dip to the W-SW (Fig. 2). These limestones intercalate thin lenses of marl, some centimeters thick and several meters in lateral extent. One of these lenses, 20–50 cm above the base of the rudstones also yielded angiosperm remains. Bivalve fragments are the main components in the rudstones/grainstones with small benthic foraminifers as minor components and up to 25% of quartz grains. Shell fragments generally show a concordant convex-up orientation. Both rudstones-grainstones and marls are locally densely bioturbated by *Sinusichnus sinuosus* and *Bichordites* (Beláustegui et al., 2014).

4.2. The fossiliferous bed

Seagrass remains appear in two marl beds in the pinnacle section, although the abundance is higher and the preservation better in the lower one. A marl bed exposed in another preserved pinnacle 90 m to the southwest of the study section also contains some seagrass fossils. The bed with the highest fossil plant concentration is a 10–16 cm thick and consists of marl with very scarce, thin and laterally discontinuous

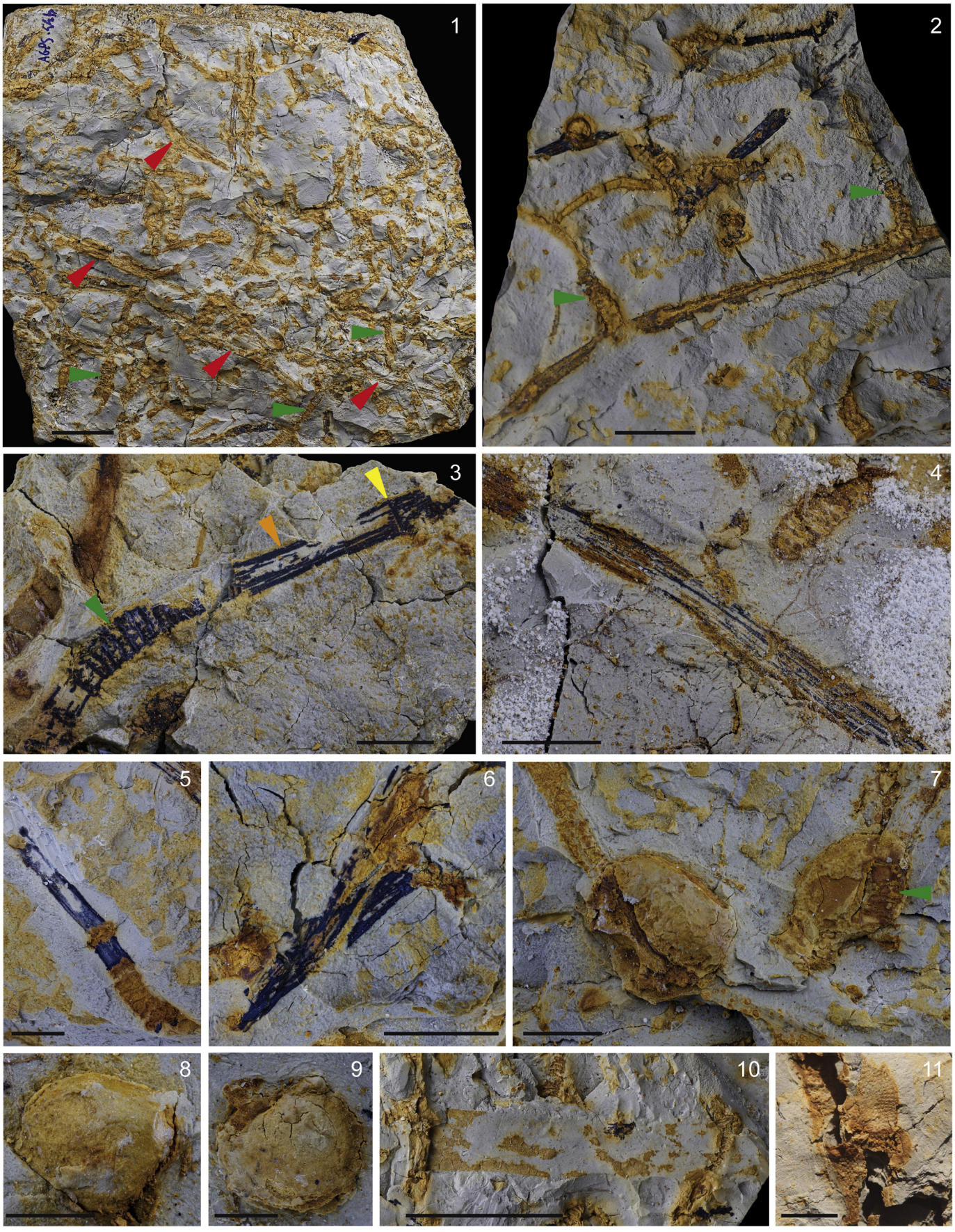
1
2
3
4
5
6
7
8
9
10
11

laminae of bioclastic sand. The marl is composed of smectite clays, quartz and calcite, with minor amounts of illite and kaolinite clays and Fe hydroxides. Angiosperm fossils appear as impressions of plant fragments from millimeters to centimeters (rarely more than 10 cm) in size (Plate I, 1–10) with diverse degrees of preservation conditioned by alteration of marl. Thin films of Fe hydroxides, and varying amounts of Fe and Mn oxides in some samples appear in the impressions (Plate I, 1–11). Several potential molds of fruits were also found (Plate I, 7–9). Fossil angiosperms occur at different levels within the bed but their concentration is higher at a surface in the middle (Plate I, 1). All plant remains except two (Plate I, 10) seem to belong to a single species of marine angiosperm. Bioturbation locally disturbs the plant preservation. In a few cases, impressions of epiphytic bryozoans were observed (Plate I, 11).

4.3. Systematic description

Order: Alismatales Dumortier, 1829
Family: Cymodoceaceae Vines, 1895
Genus: **Cymodocea** K.D. König, 1805
Type species: Cymodocea nodosa (Ucria) Ascherson, 1870
Cymodocea cf. *nodosa* (Ucria) Ascherson, 1870
Plate I, 1–9

Description: The most abundant remains are horizontal (plagiotropic) rhizomes, 3–5 mm wide (mean 3.9, standard deviation 0.5 mm) with nodes from which vertical (orthotropic) rhizomes arise (Plate I, 1,2). Observable separation of nodes (internode length) is 10.5–36 mm (Plate I, 2). No roots have been recognized. Vertical rhizomes are also common and typically show a series of nodes (leaf scars) separated by internodes 1–1.8 mm long (Plate I, 2,3,5). Vertical rhizomes are 2.8–5.2 mm wide (mean 3.7, sd 0.5 mm) and up to 30 mm long. Leaf sheaths arising from vertical rhizomes are scarce, 2.8–3 mm wide and up to 13.2 mm long (Plate I, 3, 5). Only in one case the base of a leaf in connection with the sheath at a ligule can be clearly observed (Plate I, 3). Leaves are scarce as well, elongated, ribbon-shaped with 7–9 observable nerves (Plate I, 4, 6). Leaves are 2.7–2.9 mm wide and the longest recorded remain is 40 mm long. No leaf tips have been recognized. Internal molds of pericarps are semicircular in outline and 6–10.5 mm long (Plate I, 7–9).

Remarks: Vegetative characteristics can be used in the identification of species and genera of seagrasses (Kuo and den Hartog, 2001; den Hartog and Kuo, 2006). In the study assemblage, despite the absence of flower remains, the vegetative characters preserved can be used for a confident identification of *Cymodocea*. The strap-shaped leaves developing on top of vertical rhizomes with many nodes, as well as leaves differentiated in a sheath and a blade with a ligule and with 3-many nerves are characteristic of the family Cymodoceaceae (Kuo and den Hartog, 2001; den Hartog and Kuo, 2006). The combination of monopodial horizontal rhizomes with single short vertical rhizomes in nodes, and flat leaves with 7 or more longitudinal veins are typical of *Cymodocea* (Kuo and den Hartog, 2001; den Hartog and Kuo, 2006). The occurrence of only 7–9 veins differentiates *C. nodosa* from the other *Cymodocea* species, which are distributed in the Indo-West Pacific (Kuo and den Hartog, 2001). Closed circular sheath scars in vertical rhizomes are typical of *C. nodosa* as well, although *Cymodocea rotundata* also presents this character (Kuo and den Hartog, 2001). The thickness of the impressions of horizontal and vertical rhizomes falls well within the variability of this species (Reyes, 1993, 2011; Terrados and Marbà, 2004), particularly taking into account that cylindrical rhizomes of living plants underwent compression that modified their diameters to fossil rhizome widths. According to the degree of compression the resulting width value is from 1 (no compression) to 1.57 (total compression to a plane) times the original diameter. Length of vertical rhizomes, sheath and leaf widths are also in accordance with values of living *C. nodosa* plants (Reyes, 1993, 2011; Terrados and Marbà, 2004). Nevertheless, the absence of flowers and better-preserved fruits implies a certain degree of uncertainty in the species assignment of the remains. In addition, the size of fruits (Plate I, 7–9) is smaller than that of living *C. nodosa* (Reyes, 1993, 2011; Reyes et al., 1995; Terrados and Marbà, 2004; Moreno and Guirado, 2006).

ALISMATALES indet.
Plate I, 10

Description: Two fossils of a different seagrass taxon consist of impressions of leaf fragments with iron hydroxides and manganese oxide. The best preserved one (Plate I, 10) is 4.5 cm long and 0.8 cm wide. Leaves show ribbon shapes and poorly defined longitudinal nerves.

Remarks: The leaf width clearly distinguish these fragments from the rest of seagrass fossils examined. Similar broad, strap-shaped leaves can be found in several genera belonging to different families within Allismatales, such as *Zostera* and *Posidonia*. However, no preserved characters allow a more precise identification at the genus or family level.

5. Discussion

5.1. Paleoenvironmental interpretation

The main deposits in the study section and adjacent pinnacles, trough cross-bedded grainstones to rudstones, formed in submarine dunes moved by tractive currents. The concordant convex-up orientation of shells in the beds also indicates current action (Kidwell and Bosence, 1991). The predominant dip direction to the W-SW is compatible with a littoral drift roughly parallel to the southern margin of the Guadalquivir Basin. The amalgamated lenses of rudstones with erosive bases, rough normal gradation and sharp shell fragments can be interpreted as proximal storm deposits (Aigner, 1985; Einsele and Seilacher, 1991).

Lithology, sedimentary structures and fossil assemblages indicate that the fossiliferous beds formed in a shallow-water, open marine environment, with a seafloor covered by submarine dunes mainly fed by bioclastic particles. Macroinvertebrate assemblages (Table 1) and small but significant proportions of planktonic foraminifers support the open nature of the environment. The marl lenses probably accumulated in the relatively ephemeral and small interdune lows sheltered by dunes. The baffling effect of seagrasses presumably contributed to the low turbulence at the seafloor promoting marl deposition. The pinching out of marl lenses between trough cross-bedded grainstones/rudstones indicates that the marls formed on and were covered by moving dunes.

Plate I. *Cymodocea* cf. *nodosa* and Alismatales indet. 1, *Cymodocea* cf. *nodosa* impressions partially coated/filled by Fe hydroxides (brown colored) and mixtures of Fe and Mn oxides (black colored). Concentration of fossil fragments of plagiotropic (red arrowheads) and orthotropic (green arrowheads) rhizomes at a surface in the middle of the fossiliferous marl bed, GDA-Fanero 68311. Scale bar = 20 mm. 2, Plagiotropic rhizome of *Cymodocea* cf. *nodosa* with two orthotropic rhizomes (green arrowheads) delimiting an internode, and other plant fragments. The right-hand orthotropic rhizome gives way to a poorly preserved sheath or sheath and leaf, GDA-Fanero 68307. Scale bar = 10 mm. 3, Orthotropic rhizome of *Cymodocea* cf. *nodosa* (green arrowhead) with sheath (orange arrowhead) and base of a leaf separated by a ligula (yellow arrowhead), GDA-Fanero 68310. Scale bar = 5 mm. 4, Leaf impression of *Cymodocea* cf. *nodosa*, GDA-Fanero 68304. Scale bar = 5 mm. 5, Orthotropic rhizome with sheath and leaf? of *Cymodocea* cf. *nodosa*; no defined ligula can be observed, GDA-Fanero 68309. Scale bar = 5 mm. 6, Potential leaf bundle of *Cymodocea* cf. *nodosa*; at least two leaves are superimposed and converging to their bottom left end, GDA-Fanero 68316. Scale bar = 5 mm. 7, Molds of two pericarps attached to rhizomes of *Cymodocea* cf. *nodosa*. The right-hand one is associated with an orthotropic rhizome (green arrowhead), GDA-Fanero 68314. Scale bar = 5 mm. 8, Incomplete mold of pericarp of *Cymodocea* cf. *nodosa*, GDA-Fanero 68301. Scale bar = 2 mm. 9, Mold of pericarp of *Cymodocea* cf. *nodosa*, GDA-Fanero 68317. Scale bar = 2 mm. 10, Alismatales indet., this leaf impression is wider than the majority of remains in the fossiliferous bed, GDA-Fanero 68306–2. Scale bar = 20 mm. 11, Mold of an epiphytic colony of bryozoans, GDA-Fanero 68316. Scale bar = 5 mm.

Growth of seagrass patches is common in submarine dune fields (e.g. Marbá and Duarte, 1995). The benthic foraminifer assemblage in the marls, dominated by *Elphidium*, *Biasterigerina* and *Lobatula* (Table 1), is typical for seagrass beds (Langer, 1993; Mateu-Vicens et al., 2010, 2014; Frezza et al., 2011). The depositional setting was episodically affected by storms that removed and redeposited loose sediment concentrating invertebrate fossils.

5.2. Paleobiogeography

In the late Miocene, the Guadalquivir Basin was a large embayment of the Atlantic Ocean (Esteban et al., 1996). By the late Messinian, no direct connections with the Mediterranean Sea through the Betic Cordillera were still active and the basin only opened to Atlantic in the Gulf of Cádiz area (Martín et al., 2014). This area is part of the present-day dispersion area of *Cymodocea nodosa*, which in addition to the Mediterranean Sea extends in the eastern Atlantic coasts from southern Portugal to Senegal (Global Biodiversity Information Facility, 2020). Therefore, the occurrence of *Cymodocea* cf. *nodosa* in the Guadalquivir Basin does not indicate any larger distribution area of the genus in the late Miocene. In contrast, *Cymodocea*, which is a genus of tropical affinities (Den Hartog and Kuo, 2006; Larkum et al., 2018) was present in much higher latitudes in Europe (northern France, southern England) (Reich et al., 2015 and references therein) in the warmer early and middle Eocene times (Zachos et al., 2001; Westerhold et al., 2020). The eastward connection of the Mediterranean with the Indian Ocean was closed millions of years before the late Miocene (Rögl, 1998; Bialik et al., 2019), consequently, the marked biogeographic separation of *C. nodosa* lineage from the rest of *Cymodocea* species, which have a tropical Indo-Pacific distribution, had already taken place when the Alcalá de Guadaíra *Cymodocea* plants lived.

5.3. Exceptionality of seagrass macrofossils

Despite the increasing number of records, fossils of seagrasses are sparse and always represent cases of exceptional preservation. The little or no lignification of the xylem in seagrasses (Kuo et al., 2018; Kuo and den Hartog, 2001) highly reduces the fossilization potential of these herbaceous plants. In addition, the shallow habitats of open marine grasses generally entail relatively high turbulence and, consequently, oxygenated, coarse-grained sediments that do not favor plant preservation. The fossil seagrasses from Alcalá de Guadaíra are the only known Miocene records in Europe up to now, although indirect indicators suggest that seagrasses were widespread in shallow marine environments in the Mediterranean Basin and Paratethys (Reich et al., 2015). The unique plant preservation in this site might be due an unusual deposition of marl lenses in small low-energy areas among submarine dunes that probably sheltered them. In beds with fossil plants, the lateral displacement of dunes probably covered the ephemeral marl lenses and seagrass meadows in relatively short times, preventing the development of bioturbation that would have destroyed the plant remains.

Declaration of Competing Interest

The authors declare that they have no known competing financial interests or personal relationships that could have appeared to influence the work reported in this paper.

Acknowledgments

This work was supported by Junta de Andalucía (Spain) Research Group RNM 190. Funding for open access charge: Universidad de Granada/CBUA. We are grateful to Manuel Vicente Maestre Galindo for his helpful comments during development of this research and to Francisco González Portillo and Lola Molina for their help with macrophotography. We thank Isabel Sánchez-Almazo and Nicolás Velilla for carrying out the elemental and XR analyses of fossil samples, respectively.

References

Aguirre, J., Braga, J.C., Martín, J.M., Puga-Bernabéu, A., Pérez-Asensio, N., Sánchez-Almazo, I.M., Génio, L., 2015. An enigmatic kilometer-scale concentration of small mytilids (Late Miocene, Guadalquivir Basin, S Spain). Palaeogeogr. Palaeoclimatol. Palaeoecol. 436, 199–213.

Aigner, T., 1985. Storm depositional systems. Dynamic, stratigraphy in modern and ancient shallow-marine sequences. Lecture Notes in Earth Sciences 3. Springer-Verlag, Berlin.

Ascherson, P., 1870. Sitzungs-Bericht der Gesellschaft naturforschender Freunde zu Berlin am 16. Februar 1869. Sitzungsberichte der Gesellschaft Naturforschender Freunde zu Berlin 1869, 3–6.

Beláustegui, Z., De Gibert, J.M., López-Blanco, M., Bajo Campos, I., 2014. Recurrent constructional pattern of the crustacean burrow *Sinusichnus sinuosus* from the Paleogene and Neogene of Spain. Acta Palaeontol. Pol. 59 (2014), 461–474. https://doi.org/10.4202/app.2012.0092.

Benzecry, A., Brack-Hanes, S.D., 2008. A new hydrocharitacean seagrass from the Eocene of Florida. Bot. J. Linn. Soc. 157, 19–30.

Betzler, C., Martín, J.M., Braga, J.C., 2000. Non-tropical carbonates related to rocky submarine cliffs (Miocene, Almería, southern Spain). Sediment. Geol. 131, 51–65.

Bialik, O.M., Frank, M., Betzler, C., Zammit, R., Waldmann, N.D., 2019. Two-step closure of the Miocene Indian Ocean Gateway to the Mediterranean. Sci. Rep. 9, 8842. https://doi.org/10.1038/s41598-019-45308-7.

Brachert, T.C., Betzler, C., Braga, J.C., Martin, J.M., 1998. Microtaphofacies of a warm temperate carbonate ramp (uppermost Tortonian/lowermost Messinian, southern Spain). Palaios 13, 459–475.

Brandano, M., Tomassetti, L., Mateu-Vicens, G., Gaglianone, G., 2019. The seagrass skeletal assemblage from modern to fossil and from tropical to temperate: Insight from Maldivian and Mediterranean examples. Sedimentology 66, 2268–2296.

Cheetham, A.H., Jackson, J.B.C., 1996. Speciation, extinction, and the decline of arborescent growth in Neogene and Quaternary Cheilostome Bryozoa of tropical America. In: Jackson, J.B.C., Budd, A.F., Coates, A.G. (Eds.), Evolution and Environment in Tropical America. The University of Chicago Press, pp. 205–233.

Den Hartog, C., Kuo, J., 2006. Taxonomy and biogeography of seagrasses. In: Larkum, A.W.D., Orth, R.J., Duarte, C.M. (Eds.), Seagrasses: Biology, Ecology and Conservation. Springer, Dordrecht, pp. 1–23.

Dilcher, D., 2016. Fossil plants from the Coon Creek Formation of Tennessee. Bull. Alabama Mus. Nat. Hist. 33, 118–121.

Dumortier, B.C.J., 1829. Analyse des Familles des Plantes, avec l'indication des principaux genres qui s'y rattachent. J. Casterman, Tournay, France.

Einsele, G., Seilacher, A., 1991. Distinction of tempestites and turbidites. In: Einsele, G., Ricken, W., Seilacher, A. (Eds.), Cycles and Events in Stratigraphy. Springer-Verlag, Berlin, pp. 377–382.

Esteban, M., Braga, J.C., Martín, J.M., Santisteban, C., 1996. Western Mediterranean reef complexes. In: Franseen, E.K., Esteban, M., Ward, W.C., Rouchy, J.M. (Eds.), Models for Carbonate Stratigraphy from Miocene Reef Complexes of Mediterranean Regions. SEPM Concepts Sedimentol. Paleontol vol. 5, pp. 55–72.

Fernàndez, M., Berástegui, X., Puig, C., et al., 1998. Geophysical and geological constraints on the evolution of the Guadalquivir foreland basin, Spain. In: Mascle, A., Puigdefàbregas, C., Luterbacher, H.P., et al. (Eds.), Cenozoic Foreland Basins of Western Europe. London, Geological Society Special Publication. 134, pp. 29–48.

Frezza, V., Mateu-Vicens, G., Gaglianone, G., Baldassarre, A., Brandano, M., 2011. Mixed carbonate-siliclastic sediments and benthic foraminiferal assemblages from *Posidonia oceanica* seagrass meadows of the central Tyrrhenian continental shelf (Latium, Italy). Ital. J. Geosci. 130, 352–369.

Galán Huertos, E., Pérez Rodríguez, J.L., 1989. Geología de Sevilla y alrededores y características geotécnicas de los suelos del área urbana. Ayuntamiento de Sevilla, Sevilla, Spain.

García-Castellanos, D., Fernàndez, M., Torné, M., 2002. Modelling the evolution of the Guadalquivir foreland basin (southern Spain). Tectonics 21, 1–17.

Global Biodiversity Information Facility (GBIF), 2020. https://www.gbif.org/species/5328492.

González-Delgado, J.A., Civis, J., Dabrio, C.J., Goy, J.L., Ledesma, S., Pais, J., Sierro, F.J., Zazo, C., 2004. Cuenca del Guadalquivir. In: Vera, J.A. (Ed.), Geología de España. Geological Survey of Spain (IGME) and Geological Society of Spain (SGE), Madrid, Spain, pp. 543–550.

Iles, W.J.D., Smith, S.Y., Gandolfo, M.A., Graham, S.W., 2015. Monocot fossils suitable for molecular dating analyses. Bot. J. Linn. Soc. 178, 346–374.

Jagt, J.W.M., Deckers, M., Donovan, S.K., Fraaije, R., Goolaerts, S., van der Ham, R., Hart, M.B., Jagt-Yazykova, E.A., van Konijnenburg-van Cittert, J., Renkens, S., 2019. Latest Cretaceous storm-generated sea grass accumulations in the Maastrichtian type area, the Netherlands – preliminary observations. Proc. Geol. Assoc. 130, 590–598.

Kidwell, S.M., Bosence, D.W.J., 1991. Taphonomy and time-averaging of marine shelly faunas. In: Allison, P.A., Briggs, D.E.G. (Eds.), Taphonomy. Releasing the Data Locked in the Fossil Record. Topics in Geobiology. Plenum, New York, pp. 115–209.

König, K.D., 1805. Addition to M. Cavolini's these on *Zostera oceanica* L. Ann. Bot. 2, 91–99.

Kuo, J., Cambridge, M.L., Kirkman, H., 2018. Anatomy and Structure of Australian Seagrasses. In: Larkum, A.W.D., Kendrick, G.A., Ralph, P.J. (Eds.), Seagrasses of Australia: Structure, Ecology and Conservation. Springer, pp. 93–125.

Kuo, J., den Hartog, C., 2001. Seagrass taxonomy and identification key. In: Short, F.T., Coles, R.G. (Eds.), Global Seagrass Research Methods. Elsevier, Amsterdam, pp. 31–58.

Langer, M.R., 1993. Epiphytic foraminifera. Mar. Micropaleontol. 20, 235–265.

Larkum, A.W.D., Waycott, M., Conran, J.G., 2018. Evolution and Biogeography of Seagrasses. In: Larkum, A.W.D., Kendrick, G.A., Ralph, P.J. (Eds.), Seagrasses of Australia: Structure, Ecology and Conservation. Springer, pp. 3–29.
Laurent, L., Laurent, J., 1926. Étude sur une plante fossile des dépôts du Tertiaire marin du sud de Célèbes. Jaarb. Mijnwez. Ned. Oost-Indië 54, 169–190.
Lumbert, S.H., den Hartog, C., Phillips, R.C., Olsen, F.S., 1984. The occurrence of fossil seagrasses in the Avon Park Formation (Late Middle Eocene), Levy County, Florida. Aquat. Bot. 20, 121–129.
Marbá, N., Duarte, C.M., 1995. Coupling of seagrass (*Cymodocea nodosa*) patch dynamics to subaqueous dune migration. J. Ecol. 83, 381–389.
Martín, J.M., Puga-Bernabéu, A., Aguirre, J., Braga, J.C., 2014. Miocene Atlantic-Mediterranean seaways in the Betic Cordillera (southern Spain). Rev. Soc. Geol. Esp. 27, 175–186.
Martínez del Olmo, W., Martín, D., 2016. El Neógeno de la cuenca Guadalquivir-Cádiz (Sur de España). Rev. Soc. Geol. Esp. 29, 35–58.
Martínez del Olmo, W., Martín, D., 2019. Surcos erosivos, sistemas de trubiditas y episodios climáticos en el Tortoniense y Messiniense de la Cuenca del Guadalquivir (SO de España). Rev. Soc. Geol. Esp. 32, 97–112.
Mateu-Vicens, G., Box, A., Deudero, S., Rodríguez, B., 2010. Comparative analysis of epiphytic foraminifera in sediments colonized by seagrass *Posidonia oceanica* and invasive macroalgae *Caulerpa* spp. J. Foraminifer. Res. 40, 134–147.
Mateu-Vicens, G., Khokhlova, A., Sebastián-Pastor, T., 2014. Epiphytic foraminiferal indices as bioindicators in Mediterranean seagrass meadows. J. Foramin. Res. 44, 325–339.
Moissette, P., Koskeridou, E., Corneé, J.-J., Guillocheau, F., Lécuyer, C., 2007. Spectacular preservation of seagrasses and seagrass-associated communities from the Pliocene of Rhodes, Greece. Palaios 22, 200–211.
Moreno, D., Guirado, J., 2006. Nuevos datos sobre la floración, fructificación y germinación de fanerógamas marinas en Andalucía. Acta Bot. Malacitana 31, 51–72.
Perconig, E., 1968. Biostratigrafia della sezione di Carmona (Andalusia, Spagna) in base ai foraminiferi planctonici. Giorn. Geol. 35, 191–218.
Puga-Bernabéu, Á., Braga, J.C., Martín, J.M., 2007. High-frequency cycles in Upper-Miocene ramp-temperate carbonates (Sorbas Basin, SE Spain). Facies 53, 329–345.
Reich, S., Di Martino, E., Todd, J.A., Wesselingh, F.P., Renema, W., 2015. Indirect paleo-seagrass indicators (IPSIs): a review. Earth Sci. Rev. 143, 161–186.
Reuter, M., Piller, W.E., Harzhauser, M., Kroh, A., Roegl, F., Coric, S., 2010. The Quilon Limestone, Kerala Basin, India: an archive for Miocene Indo-Pacific seagrass beds. Lethaia 44, 76–86.
Reyes, J., 1993. Estudio de las praderas marinas de *Cymodocea nodosa* (Cymodoceaceae. Magnoliophyta) y su comunidad de epifitos en el Médano (Tenerife, Islas Canarias). PhD Thesis. Universidad de La Laguna, Spain.
Reyes, J., 2011. 5. Sebadales: explosión de biodiversidad en desiertos de arena submarinos. In: Afonso-Carrillo, J. (Ed.), Biodiversidad: explorando la red vital de la que formamos parte. Actas VI Semana Científica Telesforo Bravo. Instituto de Estudios Hispánicos de Canarias, Puerto de la Cruz, Spain, pp. 159–187.
Reyes, J., Sansón, M., Afonso-Carrillo, J., 1995. Distribution and reproductive phenology of the seagrass *Cymodocea nodosa* (Ucria) Ascherson in the Canary Islands. Aquat. Bot. 50, 171–180.
Rögl, F., 1998. Palaeogeographic Considerations for Mediterranean and Paratethys Seaways (Oligocene to Miocene). Ann. des Naturhistorischen Museums Wien 99A, 279–310.
Ruggieri, G., 1951. Segnalazione di frutti fossili di *Cymodocea major* (Cavol.) Grande. Webbia 8, 141–146.
Sanz de Galdeano, C., Vera, J.A., 1992. Stratigraphic record and paleogeographical context of the Neogene basins in the Betic Cordillera, Spain. Basin Res. 4, 21–36.
Sierro, F.J., González Delgado, A., Dabrio, C.J., Flores, A., Civis, J., 1996. Late Neogene depositional sequences in the foreland basin of Guadalquivir (SW Spain). In: Friend, P., Dabrio, C.J. (Eds.), Tertiary Basins of Spain. Cambridge University Press, Cambridge, UK, pp. 339–345.
Sola, F., Braga, J.C., Aguirre, J., 2013. Hooked and tubular coralline algae indicate seagrass beds associated to Mediterranean Messinian reefs (Poniente Basin, Almería, SE Spain). Palaeogeogr. Palaeoclimatol. Palaeoecol. 374, 218–229.
Terrados, J., Marbà, N., 2004. Características morfológicas. Las praderas de *Cymodocea nodosa*. In: Luque, Á.A., Templado, J. (Eds.), Praderas y bosques marinos de Andalucía. Consejería de Medio Ambiente, Junta de Andalucía, pp. 136–138.
Tuya, F., Betancort, J.F., Haroun, R., Espino, F., Lomoschitz, A., Meco, J., 2017. Seagrass paleo-biogeography: Fossil records reveal the presence of Halodule cf. in the Canary Islands (eastern Atlantic). Aquat. Bot. 143, 1–7.
Van der Ham, R.W.J.M., Van Konijnenburg-van Cittert, J.H.A., Indeherberge, L., 2007. Seagrass foliage from the Maastrichtian type area (Maastrichtian, Danian, NE Belgium, SE Netherlands). Rev. Palaeobot. Palynol. 144, 301–319.
Van der Ham, R.W.J.M., Van Konijnenburg-van Cittert, J.H.A., Jagt, J.W.M., Indeherberge, L., Meuris, R., Deckers, M.J.M., Renkens, S., Laffineur, J., 2017. Seagrass stems with attached roots from the type area of the Maastrichtan Stage (NE Belgium, SE Netherlands): morphology, anatomy, and ecological aspects. Rev. Palaeobot. Palynol. 241, 49–69.
Verdenius, J.G., 1970. Neogene stratigraphy of the western Guadalquivir basin (Soutern Spain). Utrecht Micropaleontol. Bull. 3, 1–109.
Viguier, C., 1974. Le Néogène de l'Andalousie nord-occidentale (Espagne). Histoire géologique du «Bassin du Bas Guadalquivir». Ph.D. Thesis. University of Bordeaux, France.
Vines, S.H., 1895. A Student's Text-Book of Botany, S. Sonnenschein & Company, London.
Westerhold, T., Marwan, N., Drury, A.J., et al., 2020. An astronomically dated record of Earth's climate and its predictability over the last 66 million years. Science 369 (6509), 1383–1387.
Zachos, J., Pagani, M., Sloan, L., Thomas, E., Billups, K., 2001. Trends, rhythms, and aberrations in global climate 65 Ma to present. Science 292, 686–693.